Theoretical Study on Structures and Stability of C_4P Isomers

Guang-tao Yu, Yi-hong Ding, Xu-ri Huang,* and Chia-chung Sun

State Key Laboratory of Theoretical and Computational Chemistry, Institute of Theoretical Chemistry, Jilin University, Changchun 130023, People's Republic of China

Received: October 8, 2004; In Final Form: December 15, 2004

The structures, energetics, spectroscopies, and stabilities of doublet C_4P isomeric species are explored at the DFT/B3LYP, QCISD, and CCSD(T) (singlet-point) levels. A total of 12 minimum isomers and 27 interconversion transition states are located. At the CCSD(T)/6-311G(2df)//QCISD/6-311G(d)+ZPVE level, the lowest-lying isomer is a floppy CCCCP **1** (0.0 kcal/mol) mainly featuring a cumulenic structure |C═C═C═C═P•|, which differs much from the analogous C_4N radical (|•C−C≡C−C≡N|). The quasi-linearity and the low bending mode of **1** are in contrast to the previous prediction. The second energetically followed isomer PC-cCCC **3** (14.9 kcal/mol) possesses a CCC ring-bonded to CP. The two low-lying isomers are separated by a high-energy ring-closure/open transition state (26.5 kcal/mol) and thus are very promising candidates for future laboratory and astrophysical detection. Furthermore, four high-energy isomers, that is, two bent isomers CCPCC **2** (68.4 kcal/mol) and CCPCC **2′** (68.5 kcal/mol) and two cagelike species **10** (56.0 kcal/mol) and **11** (67.9 kcal/mol), are also stabilized by considerable barriers. The present work is the first detailed potential energy survey of C_nP clusters and can provide useful information for the investigation of larger C_nP radicals and for understanding the isomerism of P-doped C vaporization processes.

1. Introduction

Phosphorus chemistry has received considerable attention from various aspects. One particular interest is their possible role in astrophysical chemistry. Up to now, several phosphorus-containing molecules, such as NP[1] and CP[2], have been detected in interstellar space. Experimental[3] and theoretical[4] investigations have been carried out to probe their possible production mechanism in space. An important result[5] is that larger phosphorus−carbon molecules, such as C_2P and C_3P, might exist in the molecular hot core of star-forming regions provided that oxygen atoms are not injected. Thus, the carbon and phosphorus-containing species, in particular, the form C_nP, may be of astronomical interest. C_nP can be formally considered as P-doped C_n clusters. Understanding the structural, bonding, and stability properties of C_nP clusters may be helpful for future identification of the new C- and P-containing species either in laboratory or in space and also for elucidation of the formation mechanism of the phosphorus-doped C_n materials.

Despite the potential importance, however, the C_nP series ($n \geq 2$) has received little attention.[6] Experimental investigations[6a] have suggested the existence of C_nP^- radicals by observing the signals of C_nP^- ($n = 2-7$) in a TOF mass spectrometry study. The radicals C_2P[6b] and C_3P[6c] have been theoretically studied. The linear CCP and CCCP were found to be the ground states, followed by stable three-membered ring cC_2P and four-membered ring cC_3P, respectively. For the C_4P radical, three literature reports are available. One[6d] calculated the vertical electron detachment energy of the quasi-linear $CCCCP^-$ using the MP2-based methods, suggesting the possible bending of neutral CCCCP. However, the structure of neutral CCCCP was not optimized. The others[6e,6f] found neutral CCCCP to have a linear structure with all real frequencies at the B3LYP/6-311G(d) and B3LYP/6-311+G(d) levels. Therefore, to confirm the linearity and to provide accurate spectroscopic data for future characterization, a reinvestigation on CCCCP at a higher level is still desirable, which will be reported in this paper.

Our study on C_4P has a more general goal. To our surprise, though the structures and energetics of C_nP have been studied,[6b−f] their isomerization and dissociation stabilities are completely unknown. It is well-known that in some processes, the molecular isomerism plays a very important role. On one hand, an isomer with considerable kinetic stability can have a long lifetime of existence even if the isomer has high energy. A typical example is cyanoacetylene (HC_3N), for which three isomeric forms HCCCN, HCCNC, and HNCCC have all been detected in space. Of particular interest is that HNCCC[7] lies very high (50.9 kcal/mol) above HCCCN. Then, a detailed potential energy surface (PES) survey is vital for prediction of the promising isomers to be detected. In fact, for the analogous C_4N radical, theoretical studies showed that three linear isomers CCCCN, CCCNC, and CCNCC and two three-membered rings NC-cCCC and CN-cCCC have considerable kinetic stability and may be experimentally observable.[8] On the other hand, in the gas-phase vaporization process of P-doped carbon clusters, the initially formed structure may not be lowest-energy form. So, the detailed knowledge on the C_4P PES will be useful for understanding such processes. Moreover, with smaller electronegativity than nitrogen, phosphorus has fewer trends to form strong multiple bonding than nitrogen. Instead, phosphorus may form cagelike species made of single bonds. No cagelike C_4N species has sufficient kinetic stability. The electronic structures of C_4P are expected to differ from those of C_4N. Detailed analysis on the electronic and bonding nature of C_4P isomers can provide some insight into the stability and reactivity of C_nP clusters.

2. Computational Methods

All computations are carried out using the GAUSSIAN 98[9] program package. Density functional theory (DFT) methods

* Author to whom correspondence should be addressed.

10.1021/jp045393t CCC: $30.25
Published on Web 02/05/2005

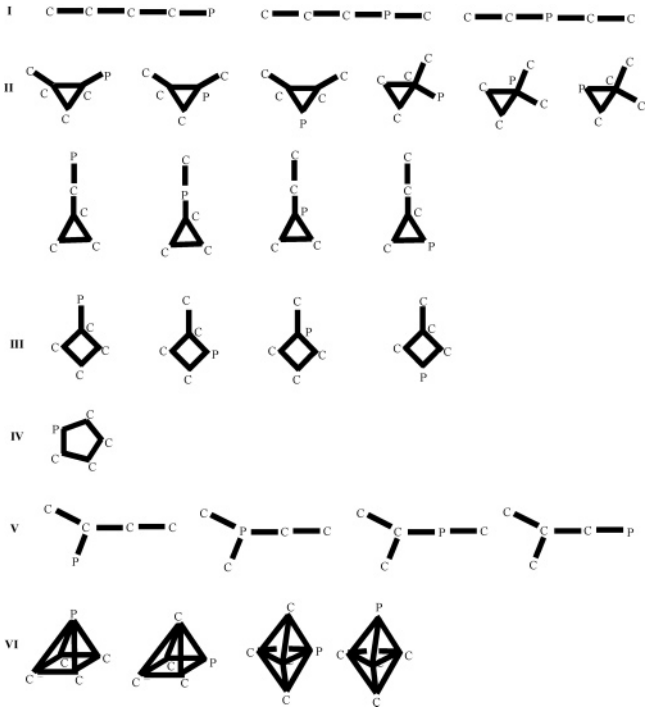

Figure 1. Scheme for isomeric species search follows.

have now been widely applied to various molecular systems with great success because of their efficiency and accuracy. In this paper, the whole potential energy surface is initially surveyed at the 6-311G(d)-B3LYP level, which includes Becke's three-parameter-exchange functionals and nonlocal Lee−Yang−Parr correlation functional. This method generally provides better results than the LSDA (local spin density approximation) and BLYP (Becke exchange functional and nonlocal LYP correlation functional) methods.[10] The optimized geometries and harmonic vibrational frequencies of the local minima and transition states are obtained at the B3LYP/6-311G(d) level. To confirm whether the obtained transition states connect the right isomers, the intrinsic reaction coordinate (IRC) calculations are performed at the B3LYP/6-311G(d) level. To get better results for relevant species, we used the quadratic configuration interaction method with single and double substitutions (QCISD) for geometries and frequencies and the coupled cluster method with single, double, and noniterative triple substitutions (CCSD(T)) for energies, respectively. Both methods represent a higher-level treatment of electron correlation beyond MP4 and can usually provide greater accuracy.[10] The basis set ranges from 6 to −311G(d) for geometry and frequency calculations to 6-311G(2d) and 6-311G(2df) for single-point energy calculations. The zero-point vibrational energies (ZPVE) at the 6-311G(d)-B3LYP and QCISD levels are included in the final relative energy consideration. For conciseness, the levels CCSD(T)/6-311G(2d)//B3LYP/6-311G(d)+ZPVE and CCSD(T)/6-311G(2df)//QCISD/ 6-311G(d)+ZPVE are simplified as CCSD(T)//B3LYP and CCSD(T)//QCISD.

3. Results and Discussions

To include as many isomeric forms as possible, we initially considered six types of isomers, that is, linear or chainlike species **(I)**, three-membered ring species **(II)**, four-membered ring species **(III)**, five-membered ring species **(IV)**, branched-chain species **(V)**, and cagelike species **(VI)**, as depicted in Figure 1.

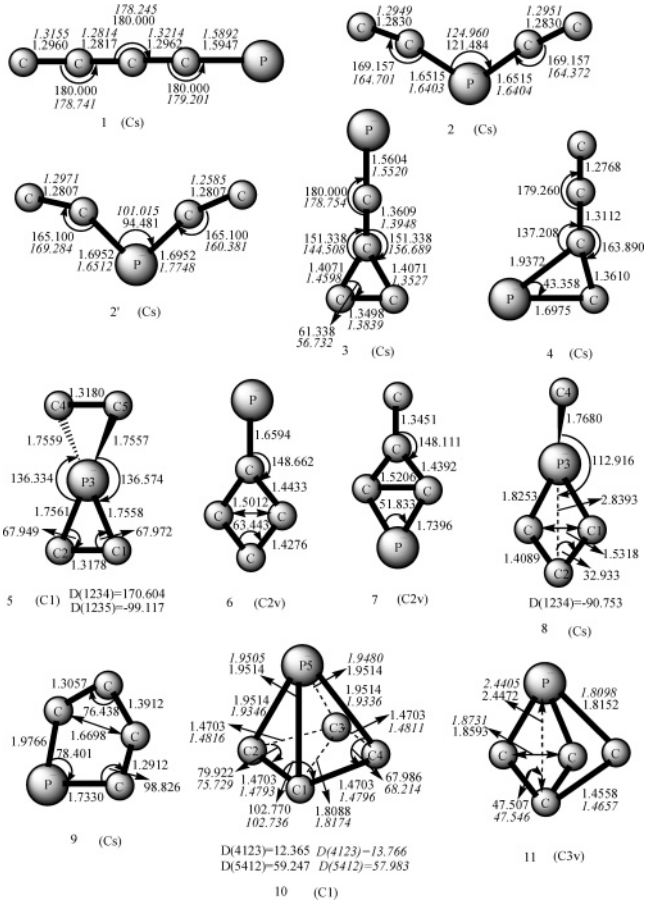

Figure 2. Optimized geometries of C_4P isomers at the B3LYP/6-311G(d) level. The values in italics are at the QCISD/6-311G(d) level. Bond lengths are in angstroms and angles are in degrees.

For conciseness, the results are organized as follows. The optimized geometries of the C_4P isomers and transition states are shown in Figure 2 and Figure 3, respectively. Optimized fragments of the dissociations of C_4P are shown in Figure 4. A schematic potential-energy surface (PES) of C_4P is presented in Figure 5. The harmonic vibrational frequencies as well as the infrared intensities, dipole moments, and rotational constants of the C_4P species are listed in Table 1, while the relative energies of all species are collected in Table 2. The relative energies of various dissociation fragments of C_4P are listed in Table 3.

3.1 C_4P Isomers. After numerous searches, 12 C_4P minimum isomers (**m**) and 27 interconversion transition states (**TSm/n**) are obtained. Among these, three isomers have chainlike structure, that is, quasi-linear CCCCP **1** (0.0), bent CCPCC **2** (66.6, *68.4*), and bent CCPCC **2′** (65.8, *68.5*). Each isomer has a $^2A'$ electronic state. The first and second (italic) values in parentheses are relative energies with reference to isomer **1** (0.0, *0.0*) at the CCSD(T)//B3LYP and CCSD(T)//QCISD levels, respectively. Notice that the present and previous[6e,6f] B3LYP/6-311G(d) and B3LYP/6-311+G(d) methods predict CCCCP **1** to be linear with the lowest bending mode about 114 cm^{-1}, as listed in Table 1. According to the assignments of each vibrational mode, the linear $^2\Pi$ structure totally has four σ-modes and six π-modes, among which the π vibrational modes are generally much weaker than the σ-modes. However, high-level QCISD/6-311G(d) calculations predict the linear $^2\Pi$ form (correlated with $^2A''$ state) to have one imaginary frequency 132*i* cm^{-1}. Relaxation of the $C_{\infty v}$ symmetry leads a slightly bent structure with ∠CCC = 178.7° and ∠CCP = 179.4°, which

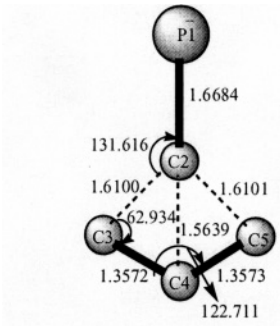

ts1/1 (C1) D(1234)=166.772
D(2345)=37.107

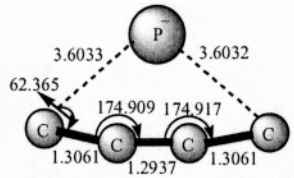

ts1/1* (Cs)

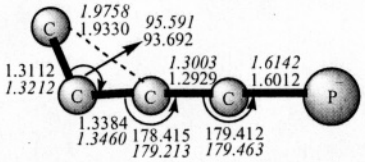

ts1/3 (Cs)

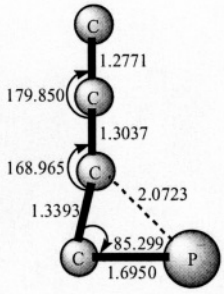

ts1/4 (Cs)

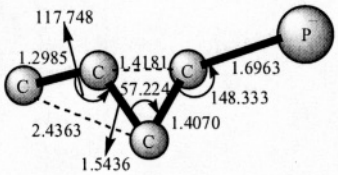

ts1/6 (Cs)

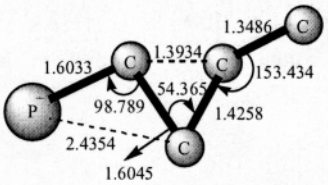

ts1/7 (Cs)

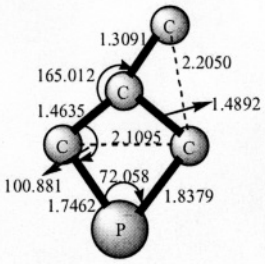

ts1/7* (Cs)

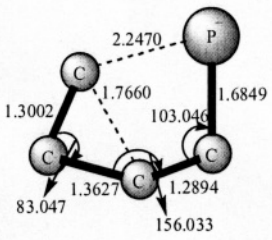

ts1/9 (Cs)

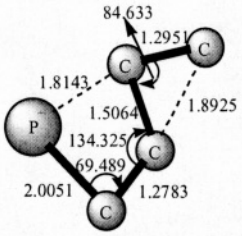

ts1/9* (Cs)

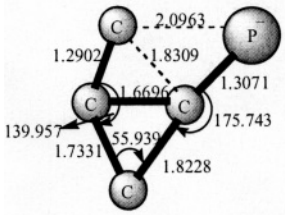

ts1/9** (Cs)

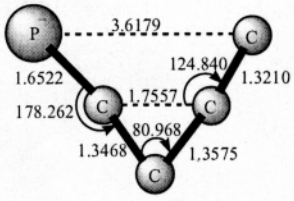

ts1/9*** (Cs)

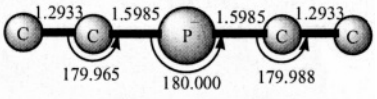

ts2/2 (Cs)

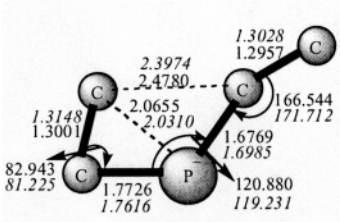

ts2/4 (Cs)

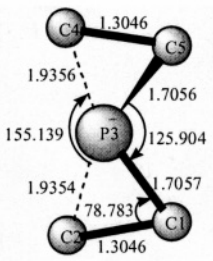

ts2/5 D(1234)=162.639
(C1) D(1235)=-54.902

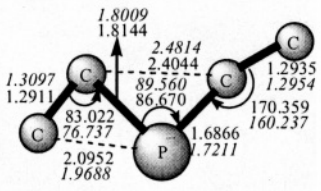

ts2'/4 (Cs)

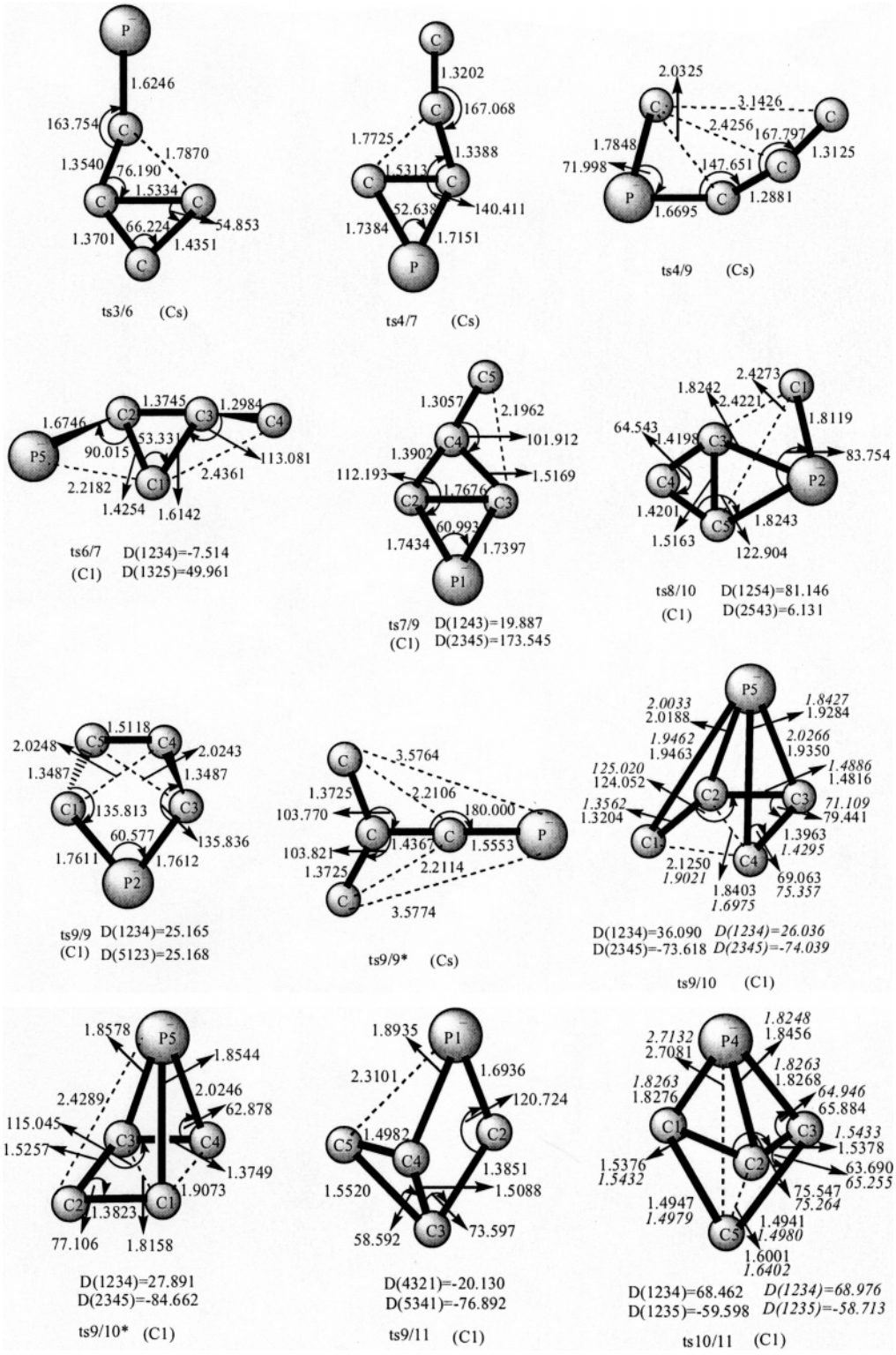

Figure 3. Optimized geometries of C_4P transition states at the B3LYP/6-311G(d) level. The values in italics are at the QCISD/6-311G(d) level. Bond lengths are in angstroms and angles in degrees.

has a $^2A'$ state. The bending mode becomes as small as 91 cm^{-1}. So, CCCCP **1** can be viewed as a floppy isomer. This is due to the Renner−Teller effect on the linear isomer CCCCP **1**. Yet such effect is minute because the nonlinearity energy is very small as 0.2 kcal/mol at the CCSD(T)/6-311G(2df)//QCISD/6-311G(d)+ZPVE level. The floppy form of **1** is also confirmed at the higher level, CCSD(T)/6-311G(3df)//QCISD/6-311G(d)+ZPVE, predicting the same nonlinearity energy 0.2 kcal/mol. As is shown, the two species **2** and **2′** with internal −P− bonding are energetically higher than the CCCCP forms. The CCCPC structure has two imaginary frequencies (206*i* and 146*i* cm^{-1}) at the B3LYP level and relaxation of its symmetry leads to the three-membered ring species **4**. Isomer **1** is a global minimum on the C_4P PES, since it contains better atomic arrangements such as −CC plus −CCP, −CCC plus −CP, or −CCCC plus P combinations.

Among the postulated three-membered ring species of type II in Figure 1, PC-cCCC **3** (13.7, *14.9*), CC-cCCP **4** (30.0), and cCCP-cPCC **5** (87.4) are located as minima. The isomers **3** and **4** have $^2A'$ states. The planar isomer **3** has a CCC three-

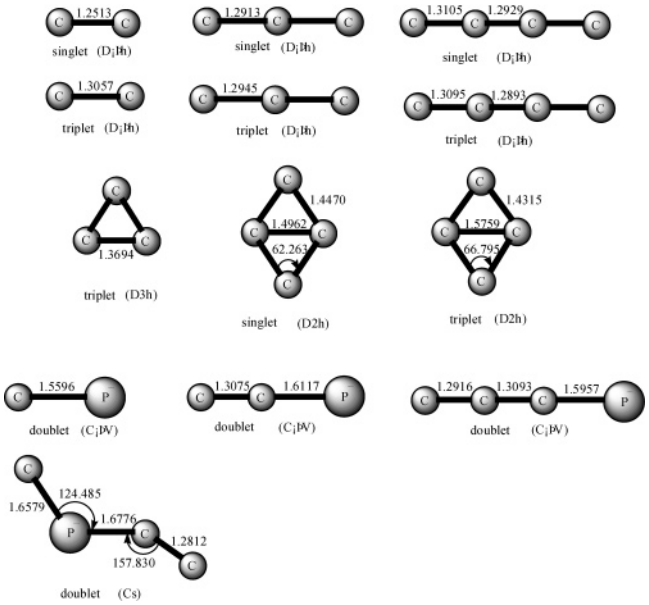

Figure 4. Optimized fragments of the dissociations of C_4P at the B3LYP/6-311G(d) level. Bond lengths are in angstroms and angles are in degrees.

membered ring with the exocyclic CP bond and it can be formally considered as the combination between the CCC ring and CP. Interestingly, isomer **3** faces a symmetry-broken problem, that is, it is of C_{2v}-symmetry at the B3LYP/6-311G-(d) level, whereas it is of C_s-symmetry at the higher QCISD/6-311G(d) level. The species **4** is a CCP-ring structure with exocyclic CCC bond, while isomer **5** is a C_1-symmetry bicyclic (two CCP-rings) structure sharing the apex P-atom. The isomer **4** can be considered as the products when the P-atom attacks the terminal π-bond of chainlike C_4. The species CP-cCCC is not minima, while the isomer CC-cPCC, which is the C_{2v} symmetry with $^2B_2$ state, has a planar imaginary frequency (141*i* cm^{-1}), and symmetric relaxation leads to the bent species **2**.

Among the postulated four-membered ring species of type III in Figure 1, P-cCCCC **6** (30.9), C-cCCPC **7** (58.4), and C-cPCCC **8** (109.2) are located as energy minima. The isomers **6** and **7** have $^2B_2$ states with C_{2v} symmetry, while the species **8** has a $^2A''$ state with C_s symmetry. The isomers **6**, **7**, and **8** possess the CCCC ring with exocyclic CP bonding, PCCC ring with exocyclic CC bonding, and CCCP ring with excyclic PC bonding, respectively. The distance between the two bridgehead C-atoms of each isomer is 1.5012 Å for **6**, 1.5206 Å for **7**, and 1.5318 Å for **8**, comparable to the typical C−C single bond (1.5297 Å in C_2H_6[11]). Orbital analysis shows the bonding nature between the two bridgehead C-atoms. Furthermore, we performed Bader's topological analysis of the charge density at the 6-311G(d)-B3LYP and MP2 levels.[12] To our surprise, only **7** has a crossed C−C bond, indicative of a bicyclic structure, whereas **6** and **8** should better be classified as monocyclic species. The species **6** may be formed when the P atom attacks either of the nonbridged C atoms of rhombic C_4. The species C-cCCCP is not minima and its optimization often leads to the isomer **1**.

Isomer **9** (45.6) is the only five-membered ring structure. The distance between two bridgehead C-atoms is as long as 1.6698 Å. Topological analysis suggests no existence of the crossed bonding. The species **9** with $^2A''$ state could be viewed as adducts of P-atom bridging to the terminus of CCCC. Among the postulated branched-chain species of type V in Figure 1, no species is a minimum. The branched-chain species CC(C)-CP has an imaginary frequency (99*i* cm^{-1}). Actually, as will be shown in the next section, it is a transition state **TS9/9*** that is associated with the automerization of the isomer **9**.

The isomers **10** (58.8, *56.0*) and **11** (72.1, *67.9*) may be seen as interesting cagelike species (type VI in Figure 1). The species **10** is a C_1-symmetry structure, while the isomer **11** has a $^2A_1$ state with C_{3v} symmetry. As shown in Figure 1, the isomer **10** is made up by four CP single bonds and four CC bonds with partial double-bonding character, while the species **11** is constitutive of six bonds with partial double-bonding character, that is, three CC and three CP bonds. Different from the C_4N[8] case, C_4P has two cagelike species **10** and **11** with relatively higher kinetic stability, that is, they are 14.7 and 10.9 kcal/mol

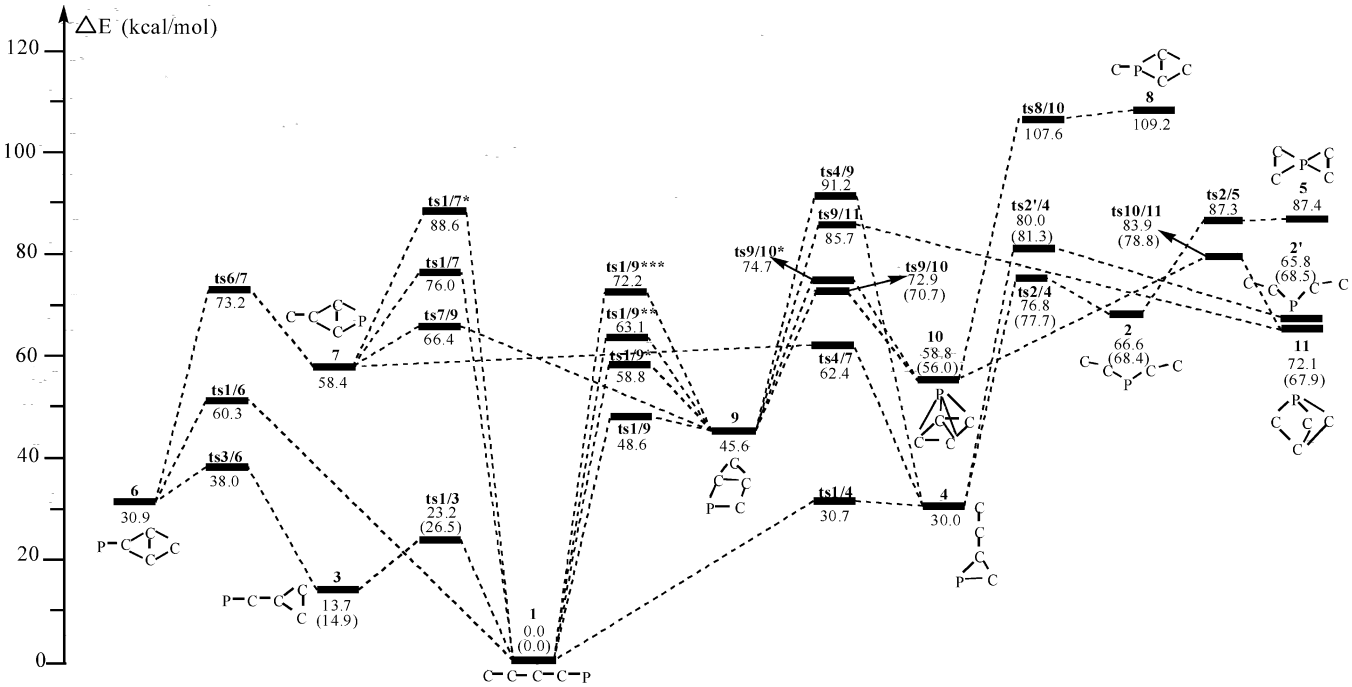

Figure 5. Schematic potential-energy surface of C_4P at the CCSD(T)/6-311G(2d)//B3LYP/6-311G(d)+ZPVE level. The relative values in parentheses are at the CCSD(T)/6-311G(2df)//QCISD/6-311G(d)+ZPVE level.

TABLE 1: Harmonic Vibrational Frequencies (cm^{-1}), Infrared Intensities (km/mol) (in Parentheses), Dipole Moment (D), Rotational Constants (GHz), and $\langle S^2 \rangle$ Values of C_4P Structures at the B3LYP/6-311G(d) Level[b]

species	frequencies (infrared intensity)	dipole moment	rotational constant	$\langle S^2 \rangle$ value
CCCCP 1	114(3,π) 129(2,π) 257(8,π) 320(7,π) 471(1,π) 581(6,π) 605(0,σ) 1215(38,σ) 1757(22,σ) 2003(846,σ)	4.4049	1.509930	0.7820
CCCCP 1[a]	91(6) 113(1) 192(0) 279(10) 309(6) 596(0) 1206(91) 1711(5) 1895(1049)	4.1790	144944.53833, 1.49010, 1.49008	1.2000
CCPCC 2	76(6) 129(0) 144(0) 172(14) 395(10) 678(1) 815(13) 1764(441) 1857(36)	2.6599	23.87502, 2.30349, 2.10080	0.7659
CCPCC 2[a]	18(0) 72(7) 82(0) 160(0) 377(9) 691(1) 828(71) 1753(1137) 1856(26)	2.5235	31.79105, 2.21171, 2.06785	0.9129
CCPCC 2′	77(12) 145(3) 186(92) 190(0) 408(11) 578(269) 767(45) 1606(36) 1790(7)	2.5309	11.51548, 2.92514, 2.33262	0.7705
CCPCC 2′[a]	98(3) 104(6) 167(0) 232(6) 419(7) 673(110) 808(3) 1737(72) 1878(607)	2.8383	13.34299, 2.66156, 2.21894	0.8423
PC-cCCC 3	104(55) 182(0) 371(320) 527(21) 552(16) 589(1) 1203(18) 1479(0) 1661(41)	3.1622	46.23242, 2.04024, 1.95401	0.7713
PC-cCCC 3[a]	162(1) 184(0) 503(16) 549(16) 582(3) 788(56) 1157(83) 1497(1) 1768(76)	3.1998	43.34146, 2.02822, 1.93755	1.3761
CC-cCCP 4	147(1) 164(8) 222(24) 465(30) 497(0) 838(1) 952(5) 1566(25) 2059(1205)	4.8600		
cCCP-cPCC 5	65(0) 154(10) 239(21) 390(108) 421(3) 621(0) 788(1) 1464(76) 1596(0)	0.0059		
P-cCCCC 6	213(3) 255(0) 527(57) 562(9) 590(0) 881(5) 1012(2) 1384(19) 1456(160)	3.2058		
C-cCCPC 7	144(2) 308(2) 461(49) 484(3) 593(0) 650(0) 982(23) 1089(5) 1501(214)	4.7995		
C-cPCCC 8	115(20) 207(1) 314(55) 386(13) 598(58) 657(71) 771(6) 949(14) 1423(4)	2.3254		
cCCCCP 9	141(3) 278(7) 337(40) 455(3) 698(5) 805(70) 1044(34) 1481(45) 1691(293)	1.5789		
cagePCCCC 10	342(12) 416(13) 468(23) 620(1) 739(0) 769(49) 844(7) 1037(90) 1210(0)	1.4533	9.85014, 7.07116, 6.05140	0.7608
cagePCCCC 10[a]	275(341) 354(18) 470(23) 650(1) 781(22) 782(41) 835(6) 1033(303) 1215(0)	1.5595	9.74263, 7.15135, 6.09572	1.3559
cageP-cCCC -C 11	343(22) 343(22) 589(18) 674(1) 674(1) 828(14) 851(12) 851(12) 1326(2)	1.9249	12.18253, 5.98306, 5.98306	0.7547
cageP-cCCC -C 11[a]	355(23) 355(23) 601(17) 698(1) 698(1) 866(16) 907(10) 907(10) 1328(4)	1.8794	12.00337, 6.00443, 6.00443	0.7778

[a] At the QCISD/6-311G(d) level. [b] For the relevant isomers, the QCISD/6-311G(d) values are included also.

TABLE 2: Relative (kcal/mol) Energies of the C_4P Structures and Transition States at the B3LYP/6-311G(d) and Single-Point CCSD(T)/6-311G(2d) Levels[a]

species	B3LYP[c]	ΔZPVE B3LYP[c]	CCSD(T) [d]//B3LYP[c]	total 1	QCISD[c]	ΔZPVE QCISD[c]	CCSD(T) [e]//QCISD[c]	total 2
CCCCP 1[b] (^{2}A′)	0.0	0.0	0.0	0.0	0.0	0.0	0.0	0.0
CCPCC 2 (^{2}A′)	74.0	−2.0	68.6	66.6	73.1	−0.8	69.2	68.4
CCPCC 2 (^{2}A′)	75.2	−2.4	68.2	65.8	65.6	−0.4	68.9	68.5
PC-cCCC 3 (^{2}A′)	18.6	−1.1	14.8	13.7	11.2	1.1	13.8	14.9
CC-cCCP 4 (^{2}A′)	34.9	−0.8	30.8	30.0				
cCCP-cPCC 5	100.8	−2.5	89.9	87.4				
P-cCCCC 6 (^{2}B$_2$)	42.4	−0.8	31.7	30.9				
C-cCCPC 7 (^{2}B$_2$)	66.6	−1.8	60.2	58.4				
C-cPCCC 8 (^{2}A″)	124.0	−2.9	112.1	109.2				
cCCCCP 9 (^{2}A″)	57.1	−0.7	46.3	45.6				
cagePCCCC 10	76.7	−1.4	60.2	58.8	63.1	0.0	56.0	56.0
cageP-cCCC-C 11 (^{2}A$_1$)	92.3	−1.4	73.5	72.1	73.7	0.5	67.4	67.9
TS1/1	80.5	−2.4	69.4	67.0				
TS1/1* (^{2}A′)	117.2	−2.5	109.5	107.0				
TS1/3 (^{2}A′)	27.1	−0.8	24.0	23.2	25.5	2.4	24.1	26.5
TS1/4 (^{2}A′)	35.1	−0.9	31.6	30.7				
TS1/6 (^{2}A′)	67.2	−1.9	62.2	60.3				
TS1/7 (^{2}A″)	86.5	−2.8	78.8	76.0				
TS1/7* (^{2}A′)	100.8	−1.4	90.0	88.6				
TS1/9 (^{2}A″)	57.8	−0.8	49.4	48.6				
TS1/9* (^{2}A″)	74.3	−2.0	60.8	58.8				
TS1/9** (^{2}A″)	78.0	−2.6	65.7	63.1				
TS1/9*** (^{2}A″)	76.0	−2.1	74.3	72.2				
TS2/2 (^{2}A′)	102.3	−2.2	97.8	95.6				
TS2/4 (^{2}A′)	88.6	−2.8	79.6	76.8	81.8	−1.4	79.1	77.7
TS2/5	102.7	−3.0	90.3	87.3				
TS2′/4 (^{2}A′)	91.5	−2.8	82.8	80.0	84.2	−1.6	82.9	81.3
TS3/6 (^{2}A′)	48.3	−1.5	39.5	38.0				
TS4/7 (^{2}A′)	70.2	−2.1	64.5	62.4				
TS4/9 (^{2}A″)	99.7	−2.4	93.6	91.2				
TS6/7	83.7	−2.3	75.5	73.2				
TS7/9	77.6	−1.8	68.2	66.4				
TS8/10	125.8	−3.1	110.7	107.6				
TS9/9	72.2	−2.2	62.7	60.5				
TS9/9* (^{2}A″)	87.0	−2.4	77.7	75.3				
TS9/10	89.0	−2.7	75.6	72.9	75.5	−1.0	71.7	70.7
TS9/10*	92.3	−3.0	77.7	74.7				
TS9/11	100.9	−2.3	88.0	85.7				
TS10/11	100.9	−2.8	86.7	83.9	83.3	−0.8	79.6	78.8

[a] For the relevant species, the values at the CCSD(T)/6-311G(2df)//QCISD/6-311G(d) are listed also. The symbols in parentheses of the column denote the point group symmetry. Only the electronic states of the species that are not of C_1 symmetry are given. [b] The total energies of reference isomer **1** at the B3LYP/6-311G(d) level are −493.5964884 au, at CCSD(T)/6-311G(2d)//B3LYP/6-311G(d) level is −492.7053341 au, at the QCISD/6-311G(d) level is −492.6276813 au, at the CCSD(T)/6-311G(2df)//QCISD/ 6-311G(d) level is −492.774298 au, and at the CCSD(T)/6-311G(3df)//QCISD/6-311G(d) level is −492.7837054 au. The ZPVE at B3LYP and QCISD level are 0.016981 and 0.014566 au, respectively. [c] The basis set is 6-311G(d) for B3LYP and QCISD. [d] The basis set is 6-311G(2d) for CCSD(T). [e] The basis set is 6-311G(2df) for the CCSD(T).

at the CCSD(T)//QCISD level, respectively, as will be discussed in the next section. Both may be experienced in P-doped carbon vaporization processes.

3.2 C_4P Isomerization and Dissociation Stability. To discuss the kinetic stability, we need to consider as many various isomerization and dissociation pathways as possible. Since the

TABLE 3: Relative (kcal/mol) Energies of Dissociation Fragments of the C_4P Structures at the B3LYP/6-311G(d) and Single-Point CCSD(T)/6−311g(2d) Levels[a]

species	B3LYP[b]	ΔZPVE B3LYP[b]	CCSD(T)[c]//B3LYP[b]	total
$C_4(^1\Pi_g) + P(^2D)$	174.2	−2.4	160.5	158.1
$cC_4(^1A_g) + P(^2D)$	172.4	−2.8	153.7	150.9
$C_4(^3\Sigma_g) + P(^2D)$	156.3	−2.5	151.4	148.9
$cC_4(^3B_{3u}) + P(^2D)$	191.9	−4.0	175.3	171.3
$C_4(^1\Pi_g) + P(^4S)$	135.6	−2.4	117.7	115.3
$cC_4(^1A_g) + P(^4S)$	133.8	−2.8	110.9	108.1
$C_4(^3\Sigma_g) + P(^4S)$	117.7	−2.5	108.6	106.1
$cC_4(^3B_{3u}) + P(^4S)$	153.3	−4.0	132.4	128.4
$C_3(^1\Sigma_g) + CP(^2\Sigma)$	121.8	−3.7	105.8	102.1
$C_3(^3\Pi_g) + CP(^2\Sigma)$	172.0	−5.3	155.9	150.6
$cC_3(^3A_1') + CP(^2\Sigma)$	140.9	−3.2	128.2	125.0
$CCCP(^2\Pi) + C(^3P)$	146.9	−3.2	134.9	131.7
$CPCC(2A') + C(^3P)$	236.1	−5.0	218.9	213.9
$CCP(^2\Pi) + CC(^1\Sigma_g)$	178.2	−3.7	139.5	135.8
$CCP(^2\Pi) + CC(^3\Pi_u)$	155.6	−3.9	141.8	137.9

[a] The symbols in parentheses of the column denote the point group symmetry. [b] The total energies of reference isomer **1** at the B3LYP and single-point CCSD(T) levels as well as the ZPVE at the B3LYP level are listed in footnote b of Table 2. The basis set is 6-311G(d) for B3LYP. [c] The basis set is 6-311G(2d) for CCSD(T).

relative energies of the dissociation products are rather high (more than 100 kcal/mol at the CCSD(T)//B3LYP level) as shown in Table 3, we do not attempt to search any dissociation transition states. So, the isomerization barriers govern the kinetic stability of C_4P isomers. For simplicity, the details of the obtained 27 transition states are omitted. We can see that the six isomers **1**, **2**, **2′**, **3**, **10**, and **11** may be of interest with relatively higher kinetic stability. The isomer **1** has considerable kinetic stability as 23.2 (*26.5*) (**1→3**) kcal/mol. Bent isomers **2**, **2′**, cyclic species **3**, and cagelike isomers **10** and **11** have slightly lower kinetic stability 10.2 (*9.3*) (**2→4**), 14.2 (*12.8*) (**2′→4**), 9.5 (*11.6*) (**3→1**), 14.1 (*14.7*) (**10→9**), and 11.8 (*10.9*) (**11→10**), respectively. The italic values in parentheses are for CCSD(T)//QCISD single-point calculations.

The other isomers have even smaller kinetic stability. At the CCSD(T)//B3LYP level, the least isomerization barriers of the species **4**, **5**, **6**, **7**, **8**, and **9** are 0.7 (**4→1**), −0.1 (**5→2**), 7.1 (**6→3**), 4.0 (**7→4**), −1.6 (**8→10**), and 3.0 (**9→1**) kcal/mol, respectively.

3.3 Properties of the Relevant Isomers. We now analyze the bonding properties of the six kinetically stable isomers **1**, **2**, **2′**, **3**, **10**, and **11** mainly on the basis of the B3LYP results. For the ground-state CCCCP **1**, its calculated terminal CC bond length (1.2960 Å) is close to the normal C═C (1.3270 Å) bond length. Its CP bond value (1.5947 Å) lies between the typical C═P (1.6702 Å) and C≡P (1.5393 Å) bond lengths. Coupled with the spin density distribution (0.357, −0.119, 0.396, −0.217, and 0.583e for C, C, C, C, and P, respectively), isomer **1** may be described as a resonance structure between (1a) |C═C═C═C═P•|, (1b) |C═C═C•−C≡P|, and (1c) |•C−C≡C−C≡P|. Form 1a bears the most weight, and 1b and 1c have comparable contribution. The symbols "•" and "|" denote the unpaired single electron and lone-pair electrons, respectively. As a result, form **1** can be generated when the combination between C_4 molecule and P-atom, or between C_3 molecule and doublet CP radical or between C_2 molecule and doublet CCP radical, takes place. For the analogous C_4N radical, the relative weight order for the valence structures of CCCCN is completely reversed as c > b > a. The difference is rationalized in that C≡P triple bonding is much weaker than C≡N bonding.

The three-membered ring PC-cCCC **3**, also the second-lowing isomer, is a C_{2v}-symmetry structure with $^2B_2$ electronic state at the B3LYP level. Its spin density distribution is 0.354, −0.184, 0.297, 0.267, and 0.267e for P, C1, C2, C3, and C4, respectively. Therefore, on the basis of the bond lengths (in Figure 2), isomer **3** can be viewed as a resonance structure between three forms:

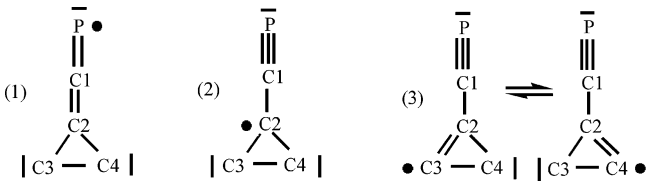

The weight of the three forms decreases from 1 to 3. Because the QCISD/6-311G(d) structure of **3** is distorted, only one form in valence structure 3 is possible. In the similar structure of C_4N radical, the contribution of the three forms is also reversed. The three-membered ring isomer **3** can be considered as the combination between the doublet CP radical and cyclic C_3 molecule.

The bend structures of the high-energy isomers CCPCC **2** and CCPCC **2′** may attribute to their internal P-atom. For the species **2**, its two terminal CC bonds lengths (1.2830 Å) are closer to the normal C═C (1.3270 Å) than to C≡C (1.1980 Å) bond values. Its two internal CP bonds values (1.6515 Å) are close to the C═P (1.6702 Å) bond length. The distribution of the spin density is 0.239, 0.097, 0.328, 0.097, and 0.239e for C, C, P, C, and C, respectively. Thus, the isomer **2** can be viewed as resonating between three forms:

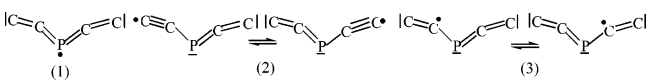

The weight of the three forms decreases from 1 to 3. Similar to isomer **2**, on the basis of the bond lengths (in Figure 1) and the spin density distribution (0.333, 0.188, −0.042, 0.188, and 0.333e for C, C, P, C, and C, respectively), isomer **2′** has a resonance structure between the above form 2 and 3. The weight of form 2 is more than form 3. Thus, we may intend to suggest that isomers **2** and **2′** can be obtained via the direct addition between CCP radical and C_2 molecule or the insertion of the P-atom into the internal C−C single bond of C_4 molecule. For the C_4N radical, the linear CCNCC indicates that the p−p overlap between nitrogen and carbon is much more effective than that between phosphorus and carbon.

The cagelike isomer **10** has the C_{2v}-symmetry structure with $^2B_2$ electronic state at the B3LYP level. Structurally, it can be

considered as P-atom interacting with all the four C-atoms of the cyclic C_4 molecule. Its CP bond lengths (1.9514 Å) are a little longer than C−P (1.8722 Å) bond values. Its peripheral CC bond values (1.4703 Å) are closer to C−C (1.5297 Å) than C═C (1.3270 Å) bond values, while the CC cross bond length (1.8088 Å) is longer than C−C (1.5297 Å) bond length. The distribution of the spin density is −0.008, 0.505, −0.001, 0.505, and −0.001e for P, C1, C2, C3, and C4, respectively. Therefore, isomer **10** can be viewed as a resonance structure between two forms:

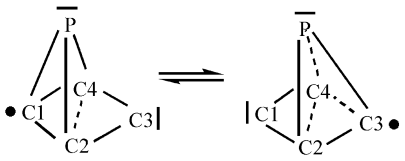

On the basis of the valence structure, the phosphorus in **10** is still of the normal tri-coordination.

The interesting cagelike isomer **11** is a C_{3v}-symmetried structure with $^2A_1$ state. The three peripheral CP bond lengths (1.8593 Å) are a little shorter than C−P (1.8722 Å) bond values. Its C1C4, C2C4, and C3C4 bond values (1.4558 Å) are closer to C−C (1.5297 Å) than C═C (1.3270 Å) bond values, suggestive of some double-bonding character. Yet, the three identical C1C2, C2C3, and C3C1 bond lengths (1.8593 Å) are much longer than typical C−C (1.5297 Å) single-bond value, which results from the high ring strain within this cage. The distribution of the spin density is 0.145, 0.039, 0.039, 0.039, and 0.739e for P, C1, C2, C3, and C4, respectively, indicating that isomer **11** can be mainly described as a following form:

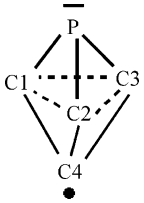

The unpaired single electron is mainly localized on the apex C4-atom.

The similar structures of **10** and **11** were also found as energy minima for the C_4N[8] radical. They were found to have much smaller kinetic stability (6.5 and 4.4 kcal/mol) toward conversion lower-energy isomers. This results from the fact that the tendency to form C−N single-bonding is much less than to form C−P single-bonding.

3.4 Interstellar and Laboratory Implications. Of the C_nP series, the simplest CP[2] radical was long known to exist in space. The C_2P and C_3P species have been suggested[5] to be generated in the molecular hot core of star-forming regions provided that oxygen atoms are not injected. Thus, it is reasonable to postulate that formation of the two low-lying isomers **1** and **3** of the C_4P radical is also probable in the same situation. Furthermore, because the fragments[2,13] CP, C_2, and C_3 have been detected in interstellar space, the direct addition between C_3 and CP or between C_2 and CCP may form the isomers **1**, **2**, and **2′**. The cyclic C_3H[13] radical has already been found in space. Replacement of the hydrogen by the CP radical is feasible to form the ring isomer PC-cCCC **3**. Indeed, the C_5H radical with a CCC ring has been successfully detected in laboratory.[14] The structures, vibrational frequencies, dipole moments, and rotational constants at the QCISD/6−311G(d) level, which are hitherto the most accurate values for C_4P, are provided in Table 1. A notable and attractive feature of the C_4P radical for the astrophysical detection is that the isomers CCCCP **1** and PC-cCCC **3** have rather large dipole moments as 4.1790 and 3.1998 D, respectively, making them very promising for microwave detection. Yet for CCCCN and NC-cCCC, the corresponding values are as small as 0.0737 and 0.6952 D.[8] Of course, the infrared characterization is also feasible for **1** and **3**.

Alternatively, all the six C_4P isomers **1**, **2**, **2′**, **3**, **10**, and **11** can be generally viewed as adducts formed by P-atom attacking the C_4 molecules. The C_4 species in both linear and cyclic forms have been characterized in laboratory.[15] During the P-doped C vaporization processes, production of the six C_4P isomers is possible via the fragment combinations, that is, C_4+P, C_3+CP, and C_2+C_2P.

The cagelike species **10** and **11** with considerable kinetic stability are of special interest. They still lie in high energy because of the high strain within the C_4P cage. However, for larger C_nP radicals or C_nP_m species, such cage structures could play an important part when the molecular space is large enough to relax the strain.

The B3LYP-based CCSD(T)/6-311G(2d) relative energies for both isomers and transition states are generally in good agreement with the QCISD-based CCSD(T)/6-311G(2df) values, as shown in Table 2.

Finally, we consider the spin contamination of the wave functions here. As shown in Table 1, the $\langle S^2 \rangle$ values at the B3LYP/6-311G(d) level are very close to the expected value 0.75 for a pure doublet state, indicative of negligible spin contamination. Yet, the $\langle S^2 \rangle$ values of the referenced Hartree−Fock wave functions in the QCISD calculations are much greater than 0.75, as is similar to the situation of the C_2P radical.[6b] The exact QCISD (or CCSD)-based wave functions are subject to little spin contaminations.

4. Conclusions

A detailed potential-energy surface of C_4P is theoretically established, involving 12 minimum isomers and 27 interconversion transition states at the B3LYP, QCISD, and CCSD(T) (single-point) levels. The main results can be summarized as follows:

(1) The lowest-lying isomer is the quasi-linear CCCCP **1** (0.0 kcal/mol) with the dominant cumulenic structure |C═C═C═C═C═P•|. Previous B3LYP calculations predict a linear form and larger bending mode. The second low-lying isomer is the three-membered ring PC-cCCC **3** (14.9) with a distorted C_3 ring. Both species **1** and **3** have considerable kinetic stability and could be observed in laboratory and in interstellar space.

(2) Four high-energy isomers, that is, bent CCPCC **2** (68.4), bent CCPCC **2′** (68.5), cagelike **10** (56.0), and cagelike **11** (67.9), also possess considerable kinetic stability. Together with the lower-energy ones **1** and **3**, they can be produced during the thermal vaporization process of phosphorus-doped carbon clusters. They can finally isomerize to **3** and **1**.

(3) Significant discrepancies are found in the bonding nature and dipole moments between C_4P and its nitrogen-analogue C_4N, which are accounted for by the different preference to form multiple-bonding or single-bonding.

(4) The present work is the first report on a detailed potential energy surface of C_nP ($n \geq 2$) radicals. It is expected to provide useful information for future investigation of larger C_nP ($n > 4$) radicals and for understanding the mechanism of P-doped carbon clusters..

Acknowledgment. This work is supported by the National Natural Science Foundation of China (No. 20073014, 20103003),

Doctor Foundation of Educational Ministry, Excellent Young Teacher Foundation of Ministry of Education of China, and Excellent Young Foundation of Jilin Province. The authors are greatly thankful to the reviewers' invaluable comments.

References and Notes

(1) (a) Turner, B. E.; Balley, J. *Astrophys. J.* **1987**, *321*, L75. (b) Ziurys, L. M. *Astrophys. J.* **1987**, *321*, L81.

(2) Guelin, M.; Cernicharo, J.; Pauber, G.; Turner, B. E. *Astron. Astrophys.* **1990**, *230*, L9.

(3) (a) Thorne, L. R.; Anicich, V. G.; Huntress, W. T., Jr. *Chem. Phys. Lett.* **1983**, *98*, 162. (b) Thorne, L. R.; Anicich, V. G.; Prasad, S. S.; Huntress, W. T., Jr. *Astrophys. J.* **1984**, *280*, 139. (c) Smith, D.; McIntosh, B. J.; Adams, N. G. *J. Chem. Phys.* **1989**, *90*, 6213.

(4) (a) Maclagan, R. G. A. R. *Chem. Phys. Lett.* **1989**, *163*, 349. (b) Maclagan, R. G. A. R. *J. Phys. Chem.* **1990**, *94*, 3373. (c) Largo, A.; Flores, J. R.; Barrientos, C.; Ugalde, J. M. *J. Phys. Chem.* **1991**, *95*, 170. (d) Redondo, P.; Largo, A.; Barrientos, C.; Ugalde, J. M. *J. Phys. Chem.* **1991**, *95*, 4318. (e) Largo, A.; Flores, J. R.; Barrientos, C.; Ugalde, J. M. *J. Phys. Chem.* **1991**, *95*, 6533. (f) Lopez, X.; Ugalde, J. M.; Barrientos, C.; Largo, A.; Redondo, P. *J. Phys. Chem.* **1993**, *97*, 1521. (g) Turner, B. E.; Tsuji, T.; Balley, J.; Guelin, M.; Cernicharo, J. *Astrophys. J.* **1990**, *365*, 569.

(5) Millar, T. J. *Astron. Astrophys.* **1991**, *242*, 241.

(6) (a) Huang, R. B.; Wang, C. R.; Liu, Z. Y.; Zheng, L. S.; Qi, F.; Yu, S. Q.; Zhang, Y. W. *Z. Phys. D* **1995**, *33*, 49. (b) Largo, A.; Barrientos, C.; Lopez, X.; Ugalde, J. M. *J. Phys. Chem.* **1994**, *98*, 3985. (c) del Rio, E.; Barrientos, C.; Largo, A. *J. Phys. Chem.* **1996**, *100*, 585. (d) Zhan, C. G.; Iwata, S. *J. Chem. Phys.* **1997**, *107*, 7323. (e) Pascoli, G.; Lavendy, H. *J. Phys. Chem. A* **1999**, *103*, 3518. (f) Li, G. L.; Tang, Z. C. *J. Phys. Chem. A* **2003**, *107*, 5317.

(7) Kolos, R.; Dobrowolski, J. C. *Chem. Phys. Lett.* **2003**, *369*, 75.

(8) Ding, Y. H.; Liu, J. L.; Huang, X. R.; Li, Z. S.; Sun, C. C. *J. Chem. Phys.* **2001**, *114*, 5170.

(9) Frisch, M. J.; Trucks, G. W.; Schlegel, H. B. et al. *GAUSSIAN 98*, Revision A.6; Gaussian, Inc.: Pittsburgh, PA, 1998.

(10) Foresman, J. B.; Frisch, Æ. *Exploring Chemistry with Electronic Structure Methods*, 2nd ed.; Guassian, Inc.: Pittsburgh, PA, 2000.

(11) The comparative bond lengths of CH_3CH_3, CH_2CH_2, CHCH, C_6H_6, CH_3PH_2, CH_2PH, and CHP are calculated at the B3LYP/6-311G(d, p) level.

(12) Bader, R. F. W. *Atoms in Molecules. A Quantum Theory*; Clarendon Press: Oxford, 1990.

(13) Smith, D. *Chem. Rev.* **1992**, *92*, 1473.

(14) Apponi, A. J.; Sanz, M. E.; Gottlieb, C. A.; McCarthy, M. C.; Thaddeus, P. *Astrophys. J.* **2001**, *547*, L65.

(15) Blanksby, S. J.; Schroder, D.; Dua, S.; Bowie, J. H.; Schwarz, H. *J. Am. Chem. Soc.* **2000**, *122*, 7105.